Journal of Chemistry and Technologies, 2025, *33*(1), 153-159

Journal of Chemistry and Technologies

pISSN 2663-2934 (Print), ISSN 2663-2942 (Online).

journal homepage: http://chemistry.dnu.dp.ua
editorial e-mail: chem.dnu@gmail.com

UDC 542.61.547

INFLUENCE of SYNTHESIS pH on STRUCTURAL, DIELECTRIC and MAGNETIC PROPERTIES of $MnFe_2O_4$

Liliya A. Frolova[1], Dmytro Yu. Saltykov[2], Iryna V. Holub[1], Olena V. Bila[1]
[1]*Ukrainian State University of Science and Technologies, 8 Nauky Ave., Dnipro, 49005, Ukraine*
[2]*Oles Honchar Dnipro National University, 72 Nauky Ave., Dnipro, 49010, Ukraine*
Received 24 December 2024; accepted 13 January 2025; available online 15 April 2025

Abstract

Dispersed manganese ferrite particles were obtained by a combined co-precipitation method at different pH of the initial solution (7–12). The structural, morphological, optical and magnetic properties of the synthesized nanoparticles were characterized using X-ray diffraction, scanning electron microscopy, and vibrational magnetometry. The XRD results showed that $MnFe_2O_4$ has a cubic spinel crystal structure with an average crystallite size of ~14–65 nm. The presence of additional phases is observed at low pH and pH greater than 12. Ferritization significantly depends on pH, which affects the phase composition of the products and the size of the crystallites. In addition, with an increase in pH from 7 to 12, the percentage of microstresses and the density of dislocations decreases. The obtained $MnFe_2O_4$ samples exhibit ferrimagnetic properties, the highest saturation magnetization value of 56.8 Emu/g is achieved at pH 10. In addition, the coercive force changes from 5 to 50 Oe with increasing pH due to the increase in crystallite size.

Keywords: $MnFe_2O_4$; coprecipitation; acidity; ferritization.

ВПЛИВ pH СИНТЕЗУ НА СТРУКТУРНІ, ДІЕЛЕКТРИЧНІ І МАГНІТНІ ВЛАСТИВОСТІ $MnFe_2O_4$

Лілія А. Фролова[1], Дмитро Ю. Салтиков[2], Ірина В. Голуб[1], Олена В. Біла[1]
[1]*Український державний університет науки і технологій, , просп.Науки, 8, Дніпро,49005, Україна*
[2]*Дніпровський національний університет імені Олеся Гончара, просп. Науки, 72, Дніпро, 49010, Україна*

Анотація

Отримано дисперсні частинки фериту марганцю комбінованим методом співосадження за різних pH початкового розчину (7–12). Структурні, морфологічні, оптичні та магнітні властивості синтезованих наночастинок були охарактеризовані за допомогою рентгенівської дифракції, скануючої електронної мікроскопії, вібраційної магнітометрії. Результати XRD показали, що $MnFe_2O_4$ має кристалічну структуру кубічної шпінелі із середнім розміром кристалітів ~14–65 нм. Наявність додаткових фаз спостерігається за низьких pH та pH більше 12. Феритизація значно залежить від pH, який впливає на фазовий склад продуктів і розмір кристалітів. Крім того, після збільшення pH від 7 до 12 зменшується відсоток мікронапружень та густина дислокацій. Отримані зразки $MnFe_2O_4$ виявляють феримагнітні властивості, найвище значення намагніченості насичення 56.8 А м^2/кг досягається за pH 10. Крім того, коерцитивна сила змінюється від 5 до 50 Ерстед під час збільшення pH за рахунок збільшення розміру кристалітів.

Ключові слова: $MnFe_2O_4$; співосадження; кислотність; феритизація.

**Corresponding author: e-mail: 19kozak83@gmail.com*

doi: 10.15421/jchemtech.v33i1.318927

Journal of Chemistry and Technologies, 2025, *33*(1), 153-159

Introduction

Nanodispersed spinel ferrites containing polyvalent metals form a number of solid solutions and compounds, which opens up unlimited possibilities for controlling the technological properties of oxides. The Fe_3O_4-Mn_3O_4 system has been studied in detail by many researchers [1–3]. This is due to the fact that manganese ferrites are widely used in industry. For example, in microwave ovens and magnetic recording systems, for the production of hydrogen as an energy source by dehydrogenation of methane in ethylene or acetylene, photocatalysis, supercapacitors and electromagnetic absorption [5–9]. Manganese ferrite forms a mixed spinel, in which approximately 80 % is normal, 20 % is inverted, and 20 % of Mn migrates from one site to another. Therefore, the synthesis of manganese spinel ferrites has long been technologically difficult. Currently, there are many methods for the synthesis of manganese ferrite particles, such as hydrothermal, ceramic, sol-gel, co-precipitation, reverse micellization, combustion, mechanosynthesis [10–18].

Hydrophase methods allow for control of the composition, crystallinity, and morphology of particles. Such methods have been studied by many researchers and have been successfully used for the synthesis of ferrites [19–23] with a particle size of 30–50 nm at a temperature of 50 °C, which is significantly lower than in the ceramic synthesis method. Coprecipitation methods usually include several stages. The first stage is the formation of a hydroxide precipitate, the second is the formation of ferrite, which is carried out by oxidation, aging, etc.

It is obvious that the synthesis conditions significantly affect the results obtained. For example, the particle size and crystallinity can be adjusted by changing the concentration of starting materials. The nucleation and growth of primary crystals depends on the chemical composition of the solution and the deposition conditions, such as the temperature and pH of the process medium [24; 25]. Methods for the synthesis of ferrites from solutions are sensitive to pH, which affects the formation of ferrite, particle size and degree of crystallinity [26]. Therefore, pH can regulate the physical and chemical properties of ferrite.

The use of low-temperature contact non-equilibrium plasma (CNP) provides a high degree of homogeneity of the distribution of components both in the initial solution and in the formed ferrite, which ensures effective interaction between the components with the formation of a relatively integral structure and composition of ferrites. We have investigated the influence of the initial pH and conditions on the production of nano-sized ferrites of different compositions from aqueous solutions using contact non-equilibrium plasma [27].

The aim of this work is to study the influence of CNP on the process of obtaining Mn-ferrites using CNP and to study their structural and phase state using X-ray and magnetic measurements.

Experimental

The coprecipitated compounds were obtained by merging with continuous stirring the appropriate mixture of sulfate solutions with the required ratio of cations, as in ferrite. Further treatment was carried out at 30 min. The treatment process was carried out in a cylindrical reactor with an internal diameter of 45 mm and a height of 85 mm. Cooling of the reaction mixture was ensured by continuous circulation of cold water in the outer jacket. The electrodes were made of stainless steel, one of which (diameter 4 mm) was located in the lower part of the reactor, and the other (diameter 2.4 mm) was placed above the surface of the solution at a distance of 10 mm. To obtain a plasma discharge, a voltage of 1000 V was applied to the electrodes. A vacuum pump was used to reduce the pressure in the reactor. Samples were prepared at an initial pH of 7–12.2.

The concentration of Mn^{2+} in the obtained samples was determined complexometrically. The concentration of iron was determined by the permanganate method. To control the reaction, the reactor was equipped with an electrode system that included a glass electrode ESL 43-07 for measuring pH, a platinum electrode for measuring oxidation potential, and an EVL-1M3 reference electrode.

The morphology of ferrite powders and their size were studied using scanning electron microscopy. The phase composition (XRD) and structure of ferrite samples were studied using a DRON-2 X-ray diffractometer in monochromatized Co-Kα-radiation. The calculation of crystallite sizes and the degree of microstress was performed by the approximation method. The average crystallite size was estimated using the Debye-Scherrer formula.

Magnetic characteristics were determined using a vibration magnetometer.

Measurements of the complex absorption and reflection coefficient, reflection coefficient, specific absorption for ferrites were performed

Journal of Chemistry and Technologies, 2025, *33*(1), 153-159

using a setup consisting of a G4-83 generator, a S4-11 spectrum analyzer, and a biconical resonator. Measurements were performed at a frequency of 10^8–10^{12} Hz at a temperature of 20 °C.

Results and discussion

Fig. 1 shows the diffraction patterns of $MnFe_2O_4$ nanoparticles obtained at different pH. It is obvious that the relative intensities of all diffraction peaks of $MnFe_2O_4$ samples are in good agreement with the cubic spinel structure of manganese ferrite with Fd3M space group (JCPDS No. 100467). It can be seen that six different peaks in the X-ray diffraction patterns of the 3 samples, corresponding to the lattice planes (220), (311), (400), (422), (511) and (440), correspond to the cubic spinel structure, which confirms the synthesis of $MnFe_2O_4$ particles at pH=10-12. The relatively broad XRD peaks are characteristic of nanosized ferrite particles. The corresponding average crystallite size is given in Table 1. As it can be seen from Table 1, the crystallite size increases with increasing pH.

Table 1

Structural parameters of samples depending on pH

pH	L_{311}, A	L_{440}, A	L, A	M 10^{-4}, %	D_{311} 10^{10}cm^{-2}	D_{440} 10^{10}cm^{-2}	a, A
7	136	131	121	2.33	394	383	
8	164	144	204	1.88	271	165	8.3402
9	141	153	533	8.7	365	429	
10	428	615	533	6.24	39.9	26,37	8.3891
11				Amorphous			
12	472	669	591	3.38	32.9	26.35	8.4012
12,2	340	584	425	10.36	63.16	29.45	8.3891

Table 1 shows that with increasing pH, lattice parameters and crystallite size, the average value of microstrains increases, while the dislocation density shows a tendency to decrease. The increase in the percentage of microstrains at low pH is consistent with the decrease in grain size and the deviation of the lattice parameters of $MnFe_2O_4$ nanoparticles. A higher value of the dislocation density causes a decrease in lattice defects due to a decrease in grain size. It is obvious that a decrease in crystallite size leads to an increase in the specific surface area, which causes an increase in surface effects. Thus, the synthesized samples at lower pH values have a larger surface area with significant surface effects in accordance with the smaller particle size.

The analysis of the X-ray diffraction patterns also shows that the crystal lattice parameter is 8.34–8.40 Å (for stoichiometric manganese ferrite of cubic structure $MnFe_2O_4$ a = 8.47 Å). The decrease in the lattice parameter value can be explained by the redistribution of cations across the sublattices.

From Table 1, it can be seen that with increasing pH, the lattice parameters and crystallite size, the average value of microstrains increase, while the dislocation density shows a tendency to decrease. The increase in the percentage of microstrains at low pH is consistent with the decrease in grain size and the deviation of the lattice parameters of $MnFe_2O_4$ nanoparticles. A larger value of the dislocation density causes a decrease in lattice defects due to a decrease in grain size. It is obvious that a decrease in crystallite size leads to an increase in the specific surface area, which causes an increase in surface effects. Thus, the synthesized samples at lower pH values have a larger surface area with significant surface effects corresponding to a smaller particle size.

Analysis of X-ray diffraction patterns also shows that the crystal lattice parameter is 8.34–8.40 Å (for stoichiometric manganese ferrite of cubic structure $MnFe_2O_4$ a=8.47 Å). The decrease in the lattice parameter value can be explained by the redistribution of cations across sublattices.

Fig. 2 presents SEM images of synthesized $MnFe_2O_4$ nanoparticles at pH 10 and 12 to investigate their size and morphology. SEM morphological analysis shows significant agglomeration of $MnFe_2O_4$ due to the interaction between magnetic nanoparticles. This effect can be explained by the action of Van der Waals forces and magnetic interaction, which causes the formation of aggregates. This is a characteristic feature of spinel ferrites obtained under the action of CNP [26].

These observations are in good agreement with the results of X-ray phase analysis. Analysis of the two SEM images indicates that a higher pH value of =12 promotes the formation of larger particles.

Journal of Chemistry and Technologies, 2025, *33*(1), 153-159

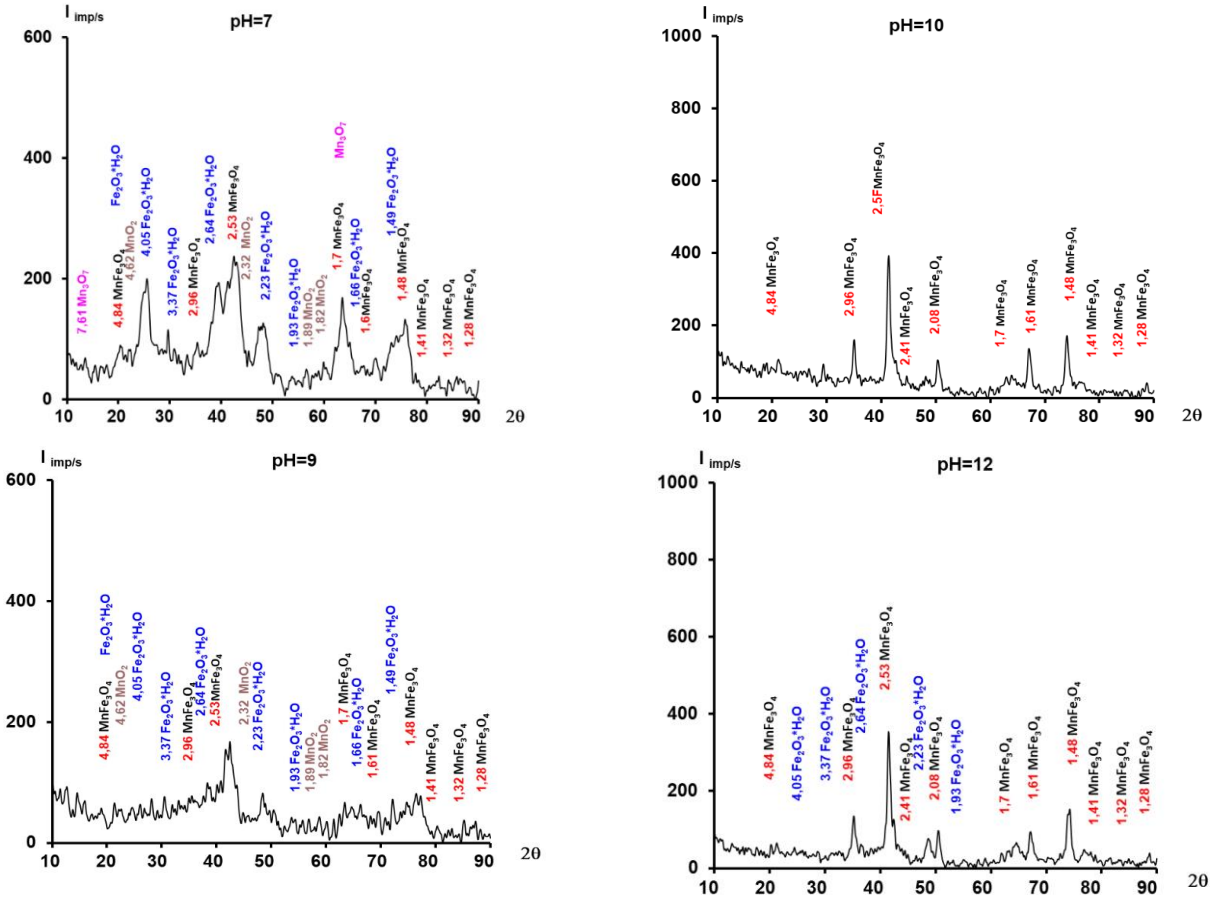

Fig. 1 X-ray diffraction patterns of samples obtained at different pH

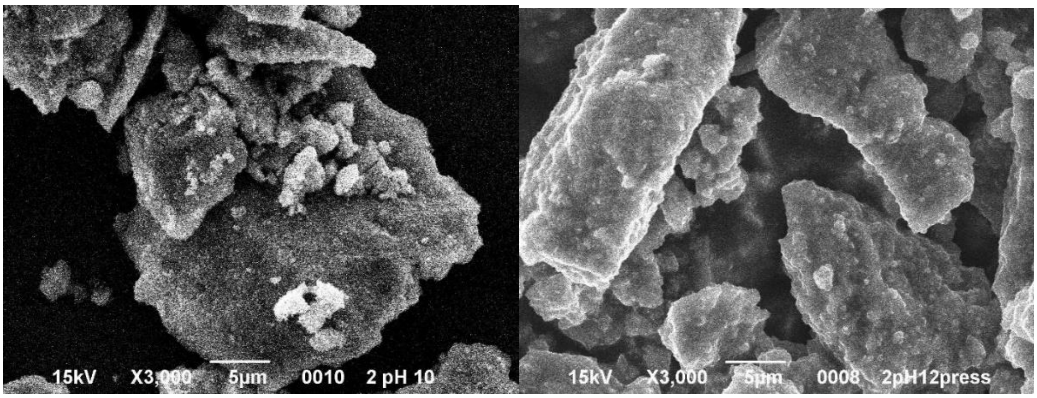

Fig. 2. SEM photographs of $MnFe_2O_4$ particles obtained at pH=10, pH=12

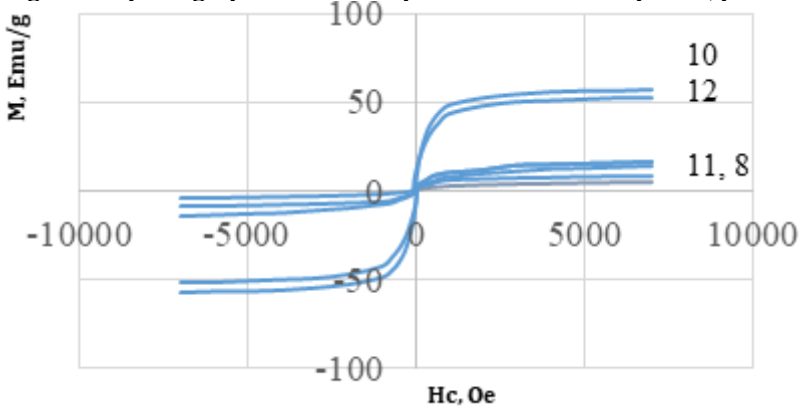

Fig. 3. Magnetic hysteresis loops for ferrites as a function of pH

Journal of Chemistry and Technologies, 2025, *33*(1), 153-159

The magnetic properties of $MnFe_2O_4$ particles with different initial pH were investigated using vibrational magnetometry at 300 K under a magnetic field of up to ±10 kOe, as shown in Fig. 3. As it can be seen from Fig. 3, four $MnFe_2O_4$ samples have almost zero coercive force and saturation residual magnetization of 8.29–16.2 Emu/g on the magnetization curve. It can also be seen that with increasing applied field, the magnetization increases and reaches almost a saturation point near the maximum applied field of 10 kOe. The saturation magnetization (Ms) is calculated from the point of intersection on the M axis of the M=f(H) plot.

At pH 7, a decrease in saturation magnetization (4.5 emu/g) is observed, which is associated with the formation of additional phases α-$Fe_2O_3 \cdot H_2O$ and MnO_2 together with the manganese ferrite phase. The highest saturation magnetization of ~56.9 Emu/g was achieved at pH 12, while a further increase in pH leads to a decrease in magnetic properties.

Fig. 4 shows the dependence of the complex absorption and reflection coefficient, reflection coefficient, specific absorption for ferrites on frequency. The reflection coefficient decreases from 0.09 to 0.07 in the range of 8–12 GHz for samples with different initial pH. The lowest values of the reflection coefficient are observed at pH 10. The specific absorption coefficient increases from 10.1 to 15.2 dB/mm.

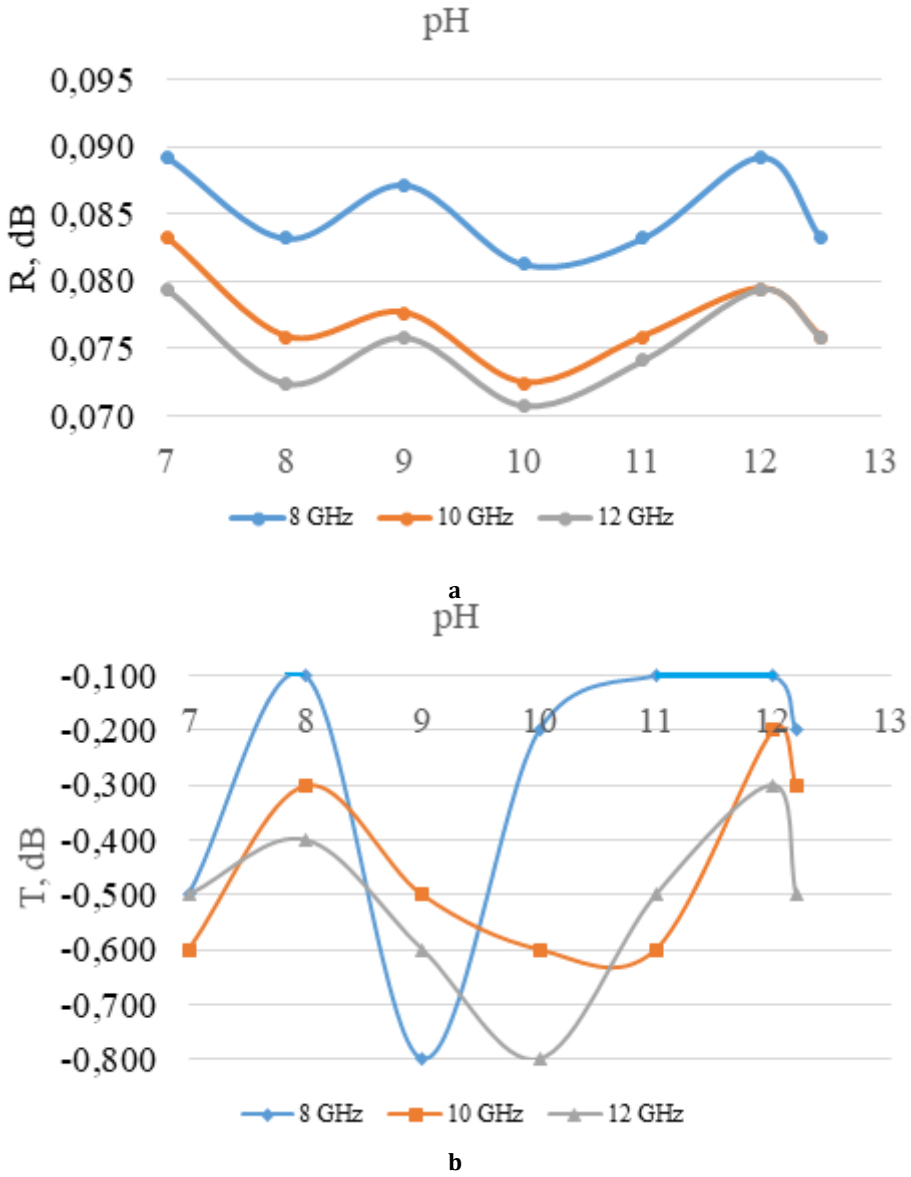

Fig. 4. Dependence of the reflection coefficient (a) and the complex reflection and absorption coefficient (b) on the frequency of electromagnetic radiation for ferrites

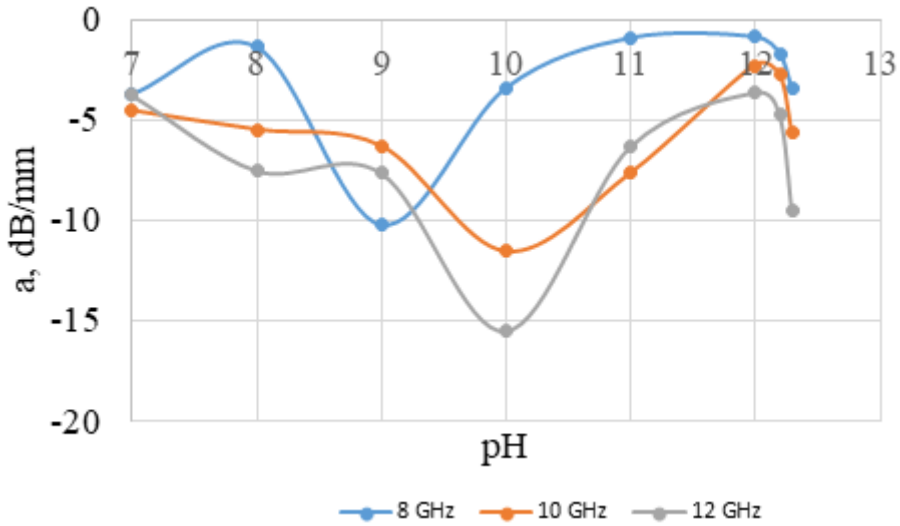

Fig. 5. Frequency dependence of electromagnetic radiation absorption for manganese ferrites at different pH

Conclusions

$MnFe_2O_4$ samples were obtained by a combined co-precipitation method at different initial pH (7–12.2) of the solution. The pH values affect the oxidation rate due to the formation of different precursors, and then affect the structure, phase composition, morphology and magnetic properties. The high oxidation rate at pH 7 leads to the formation of additional phases α-Fe_2O_3 H_2O and MnO_2 together with the manganese ferrite phase, which leads to a decrease in the saturation magnetization (4.5 Emu/g). The morphology of the powders changes, which is accompanied by an increase in the size of crystallites and agglomerates with increasing pH. The highest saturation magnetization of ~56.9 Emu/g was achieved at pH 12, while a further increase in pH leads to a decrease in the magnetic properties.

The dependence of the complex absorption and reflection coefficient, reflection coefficient, specific absorption for $MnFe_2O_4$/PVA composites on frequency and pH was determined and analyzed. The synthesized composites were fabricated and demonstrated a maximum reflection loss of 15.6 dB at 10.0 GHz with a bandwidth of approximately 1.5 GHz in a 1 mm thick sample. The results show that the composites exhibit good absorption characteristics of manganese ferrites obtained at pH 10.

References

[1] Chen, C. L., Dong, C. L., Chern, G., Kumar, K., Lin, H. J., Chen, C. T., Fujimori, A. (2014). Direct spectroscopic identification of the magnetic structure of the interface of Mn_3O_4/Fe_3O_4 superlattices. *Journal of alloys and compounds*, *614*, 177–181. https://doi.org/10.1016/j.jallcom.2014.06.074

[2] Salviano, L. B., Cardoso, T. M. D. S., Silva, G. C., Dantas, M. S. S., Ferreira, A. D. M. (2018). Microstructural assessment of magnetite nanoparticles (Fe_3O_4) obtained by chemical precipitation under different synthesis conditions. *Materials Research*, *21*, e20170764. https://doi.org/10.1590/1980-5373-MR-2017-0764

[3] Frolova, L. A., Khmelenko, O. V. (2021). The study of Co–Ni–Mn ferrites for the catalytic decomposition of 4-nitrophenol. *Catalysis Letters*, 151, 1522–1533. https://doi.org/10.1007/s10562-020-03419-1

[4] Eyvazi, B., Jamshidi-Zanjani, A., Darban, A. K. (2020). Synthesis of nano-magnetic $MnFe_2O_4$ to remove Cr (III) and Cr (VI) from aqueous solution: A comprehensive study. *Environmental Pollution*, *265*, 113685. https://doi.org/10.1016/j.envpol.2019.113685

[5] Sun, Y., Feng, J., Zhu, W., Hou, R., Zhang, B., Ishag, A. (2024). The recent advances of $MnFe_2O_4$-based nanoparticles in environmental application: A review. *Science of The Total Environment*, 176378. https://doi.org/10.1016/j.scitotenv.2024.176378

[6] Quang, N. V., Huong, P. T. L., Tu, N., Huyen, N. T., Tuan, N.T., Tran, M. T., Le, A. T. (2020). Effects of synthesis conditions on structure and magnetic properties of $MnFe_2O_4$ particles. *Green Materials*, *9*(3), 108–119. https://doi.org/10.1680/jgrma.20.00010

[7] Mazurenko, R., Prokopenko, S., Godzierz, M., Hercog, A., Makhno, S., Szeluga, U., Kartel, M. (2023). Synthesis of nanosized spinel ferrites $MnFe_2O_4$ on the surface of carbon nanotubes for the creation of polymer composites with enhanced microwave absorption capacity. *Applied Materials Today*, *35*, 101972. https://doi.org/10.1016/j.apmt.2023.101972

[8] Fei, M., Zhang, R., Li, L., Li, J., Ma, Z., Zhang, K., Yan, D. (2021). Epitaxial growth of $MnFe_2O_4$ nanosheets arrays for supercapacitor. *Electrochimica Acta*, *368*, 137586. https://doi.org/10.1016/j.electacta.2020.137586

[9] Shaw, S. K., Kailashiya, J., Gupta, S. K., Prajapat, C. L., Meena, S. S., Dash, D., Prasad, N. K. (2022). $MnFe_2O_4$ nano-flower: A prospective material for bimodal hyperthermia. *Journal of Alloys and Compounds*, *899*, 163192. https://doi.org/10.1016/j.jallcom.2021.163192

[10] Akhlaghi, N., Najafpour-Darzi, G. (2021). Manganese ferrite ($MnFe_2O_4$) Nanoparticles: From synthesis to application-A review. *Journal of Industrial and*

Engineering Chemistry, *103*, 292–304. https://doi.org/10.1016/j.jiec.2021.07.043

[11] Rafienia, M., Bigham, A., Hassanzadeh-Tabrizi, S. A. (2018). Solvothermal synthesis of magnetic spinel ferrites. *Journal of Medical Signals & Sensors*, *8*(2), 108–118.

[12] Ju, Y. W., Park, J. H., Jung, H. R., Cho, S. J., Lee, W. J. (2008). Electrospun $MnFe_2O_4$ nanofibers: preparation and morphology. *Composites Science and Technology*, *68*(7-8), 1704–1709. https://doi.org/10.1016/j.compscitech.2008.02.015

[13] Amulya, M. S., Nagaswarupa, H. P., Kumar, M. A., Ravikumar, C. R., Kusuma, K. B. (2021). Sonochemical synthesis of $MnFe_2O_4$ nanoparticles and their electrochemical and photocatalytic properties. *Journal of Physics and Chemistry of Solids*, *148*, 109661. https://doi.org/10.1016/j.jpcs.2020.109661

[14] Chen, D., Zhang, Y., Kang, Z. (2013). A low temperature synthesis of $MnFe_2O_4$ nanocrystals by microwave-assisted ball-milling. *Chemical Engineering Journal*, *215*, 235–239. https://doi.org/10.1016/j.cej.2012.10.061

[15] Popa, M., Bruna, P., Crespo, D., Calderon Moreno, J. M. (2008). Single-Phase $MnFe_2O_4$ Powders Obtained by the Polymerized Complex Method. *Journal of the American Ceramic Society*, *91*(8), 2488–2494. https://doi.org/10.1111/j.1551-2916.2008.02501.x

[16] Gao, L., Liu, Z., Yang, Z., Cao, L., Feng, C., Chu, M., Tang, J. (2020). Synthesis and magnetism property of manganese ferrite $MnFe_2O_4$ by selective reduction and oxidization roasting process. *Applied Surface Science*, *508*, 145292. https://doi.org/10.1016/j.apsusc.2020.145292

[17] Kalaiselvan, C.R., Laha, S.S., Somvanshi, S. B., Tabish, T.A., Thorat, N. D., Sahu, N. K. (2022). Manganese ferrite ($MnFe_2O_4$) nanostructures for cancer theranostics. *Coordination Chemistry Reviews*, *473*, 214809. https://doi.org/10.1016/j.ccr.2022.214809

[18] Chandunika, R. K., Vijayaraghavan, R., & Sahu, N. K. (2020). Magnetic hyperthermia application of $MnFe_2O_4$ nanostructures processed through solvents with the varying boiling point. *Materials Research Express*, *7*(6), 064002. doi 10.1088/2053-1591/ab955e

[19] Cigarroa-Mayorga, O. E. (2021). Tuning the size stability of $MnFe_2O_4$ nanoparticles: Controlling the morphology and tailoring of surface properties under the hydrothermal synthesis for functionalization with myricetin. *Ceramics International*, *47*(22), 32397–32406. https://doi.org/10.1016/j.ceramint.2021.08.139

[20] Wang, G., Zeng, Y., Zhou, F., Chen, X., Ma, Y., Zheng, L., Yu, R. (2020). One-step solvothermal synthesis of porous $MnFe_2O_4$ nanoflakes and their magnetorheological properties. *Journal of Alloys and Compounds*, *819*, 153044. https://doi.org/10.1016/j.jallcom.2019.153044

[21] Nguyen, T. D. H., Lin, M. F., Hsu, W. D. (2024). Investigations on electronic, magnetic, and optical properties of $MnFe_2O_4$ through first-principles calculations. *Computational Materials Science*, *235*, 112831. https://doi.org/10.1016/j.commatsci.2024.112831

[22] Poongodi, R., Senguttuvan, S., Sebastian, S., Sagayaraj, R. (2024). Analyzing the variations in electrical, structural and magnetic properties of zinc-doped $MnFe_2O_4$ ferrite obtained via co-precipitation. *Journal of the Australian Ceramic Society*, 1–12. https://doi.org/10.1007/s41779-024-01057-z

[23] .Simon, C., Blösser, A., Eckardt, M., Kurz, H., Weber, B., Zobel, M., Marschall, R. (2021). Magnetic properties and structural analysis on spinel $MnFe_2O_4$ nanoparticles prepared via non-aqueous microwave synthesis. *Zeitschrift für anorganische und allgemeine Chemie*, *647*(22), 2061–2072. https://doi.org/10.1002/zaac.202100190

[24] Wen, S., Chen, B., Zhang, J., Zhan, W., He, Z., Gao, L. (2023). Systematic Study on the Synthesis and Magnetism Properties of Manganese Ferrite $MnFe_2O_4$ by an Oxidation Roasting Process. *Crystals*, *13*(10), 1509. https://doi.org/10.3390/cryst13101509

[25] Frolova, L. A. (2019). The mechanism of nickel ferrite formation by glow discharge effect. *Applied Nanoscience*, *9*, 845–852. https://doi.org/10.1007/s13204-018-0767-z

[26] Frolova, L. A., Derhachov, M. P. (2017). The Effect of Contact Non-equilibrium Plasma on Structural and Magnetic Properties of $Mn_xFe_{3-x}O_4$ Spinels. *Nanoscale research letters*, *12*, 1–9. https://doi.org/10.1186/s11671-017-2268-5

[27] Frolova, L., Khmelenko, O. (2018). Investigation of the Magnetic Properties of Ferrites in the CoO-NiO-ZnO Using Simplex-Lattice Design. *Journal of Nanomaterials*, *2018*(1), 5686741. https://doi.org/10.1155/2018/5686741